A transcription factor and a phosphatase regulate temperature-dependent morphogenesis in the fungal plant pathogen Zymoseptoria tritici

Author(s):
Sardinha Francisco, Carolina; McDonald, Bruce; Palma-Guerrero, Javier

Publication date:
2023-06

Permanent link:
https://doi.org/10.3929/ethz-b-000615012

Originally published in:
Fungal Genetics and Biology 167, https://doi.org/10.1016/j.fgb.2023.103811

Fungal Genetics and Biology 167 (2023) 103811

Contents lists available at ScienceDirect

Fungal Genetics and Biology

journal homepage: www.elsevier.com/locate/yfgbi

A transcription factor and a phosphatase regulate temperature-dependent morphogenesis in the fungal plant pathogen *Zymoseptoria tritici*

Carolina Sardinha Francisco *, Bruce A. McDonald, Javier Palma-Guerrero *

Plant Pathology Group, Institute of Integrative Biology, 8092 ETH Zürich, Switzerland

ARTICLE INFO

Keywords:
Dimorphism
Zymoseptoria tritici
Heat stress
Phosphatase
Transcriptional hyphal repressor

ABSTRACT

Naturally fluctuating temperatures provide a constant environmental stress that requires adaptation. Some fungal pathogens respond to heat stress by producing new morphotypes that maximize their overall fitness. The fungal wheat pathogen *Zymoseptoria tritici* responds to heat stress by switching from its yeast-like blastospore form to hyphae or chlamydospores. The regulatory mechanisms underlying this switch are unknown. Here, we demonstrate that a differential heat stress response is ubiquitous in *Z. tritici* populations around the world. We used QTL mapping to identify a single locus associated with the temperature-dependent morphogenesis and we found two genes, the transcription factor *ZtMsr1* and the protein phosphatase *ZtYvh1*, regulating this mechanism. We find that *ZtMsr1* regulates repression of hyphal growth and induces chlamydospore formation whereas *ZtYvh1* is required for hyphal growth. We next showed that chlamydospore formation is a response to the intracellular osmotic stress generated by the heat stress. This intracellular stress stimulates the cell wall integrity (CWI) and high-osmolarity glycerol (HOG) MAPK pathways resulting in hyphal growth. If cell wall integrity is compromised, however, *ZtMsr1* represses the hyphal development program and may induce the chlamydospore-inducing genes as a stress-response survival strategy. Taken together, these results suggest a novel mechanism through which morphological transitions are orchestrated in *Z. tritici* – a mechanism that may also be present in other pleomorphic fungi.

1. Introduction

Temperature fluctuation is a ubiquitous stress that disrupts homeostasis in all organisms, including fungi. An abrupt temperature change demands a rapid re-adjustment of fungal physiology and therefore represents an environmental stress signal. Some fungal species respond to heat stress by altering their growth forms. For these fungi, temperature shifts provide decisive environmental cues that affect their development. For example, thermally dimorphic human pathogens, such as *Histoplasma capsulatum* and *Paracoccidioides brasiliensis*, grow as hyphae at ambient temperatures below 30°C and convert into the pathogenic yeast form at the elevated host temperature (Gauthier, 2017; Klein and Tebbets, 2007; Sil and Andrianopoulos, 2014). In contrast, the ambient temperature favors the yeast-like phase of *Candida albicans*, while high temperature induces filamentous growth (Sudbery, 2011). Though the morphological outcomes seem to be tightly associated with the life histories of different fungal species, the regulatory circuits controlling heat stress responses usually include the upregulation of thermal proteins (Panaretou and Zhai, 2008; Tiwari et al., 2015); changes in cellular composition (Arroyo et al., 2016; Dunayevich et al., 2018; Fillinger et al., 2001; Heilmann et al., 2013), and activation of mitogen-activated protein kinase (MAPK) signaling pathways (Fuchs and Mylonakis, 2009; Levin, 2005; Sanz et al., 2017), consistent with the idea that fungal cells have evolved shared mechanisms to cope with changing temperatures (Brown et al., 2014; Brown et al., 2017; Leach and Cowen, 2013).

MAPK signal transduction pathways link environmental changes to transcriptional regulation in many eukaryotic cells. Although the number of MAPK pathways used by filamentous fungi can vary among different species (Jiang et al., 2018; Martinez-Soto and Ruiz-Herrera, 2017; May et al., 2005; Zhao et al., 2007), they are generally conserved and play a pivotal role in regulating many physiological and developmental processes in fungi. Two of them, the cell wall integrity (CWI) and high-osmolarity glycerol (HOG) pathways, are regulated in a coordinated manner during heat stress (Dunayevich et al., 2018; Fuchs and Mylonakis, 2009; Rodriguez-Pena et al., 2010; Winkler et al., 2002).

* Corresponding authors at: Environmental Genomics Group, Botanical Institute, 24118 CAU Kiel, Germany (Carolina Sardinha Francisco). Metazoa Phylogenomics Lab, Institut de Biologia Evolutiva, Council of Scientific Research (CSIC), 08003, Barcelona, Spain. (Javier Palma-Guerrero).
E-mail addresses: csardinha@bot.uni-kiel.de (C.S. Francisco), javipalma@gmail.com (J. Palma-Guerrero).

https://doi.org/10.1016/j.fgb.2023.103811
Received 15 January 2023; Received in revised form 26 April 2023; Accepted 10 May 2023
Available online 15 May 2023

CWI is activated by perturbations of the cell surface or plasma membrane and is responsible for maintaining cell morphology (Levin, 2005). Cell sensors at the fungal plasma membrane convey cell surface signals to the nucleus through sequential phosphorylation of MAPK proteins, which in turn promote the activation of MAPK *Slt2* (homologue *Mpk1* in *Saccharomyces cerevisiae*) (Kock et al., 2015; Levin, 2005; Philip and Levin, 2001). Null mutants in the CWI pathway display altered growth, cell lysis defects, and thermosensitivity (Li et al., 2014; Madden et al., 1997; Mehrabi et al., 2006a; Navarro-García et al., 1995; Onyilo et al., 2018; Verna et al., 1997; Yago et al., 2011). HOG is a well-known regulatory pathway involved in responses to osmotic stress (Roman et al., 2020). Osmoregulation maintains an appropriate intracellular environment for biochemical reactions and fungal cell turgor by controlling the efflux and influx of osmolytes (Hohmann et al., 2007). Nevertheless, the HOG pathway is also involved in morphogenesis and cell wall biogenesis (Roman et al., 2020), two essential traits related to fungal virulence (Rooney and Klein, 2002). For instance, *Hog1* mutants in different fungal pathogens can display impaired hyphal growth or cell wall structures that lead to lower virulence (Day et al., 2018; Huang et al., 2021; Mehrabi et al., 2006b). Thus, defining the cellular machinery that controls morphological transitions at high temperatures can provide unique insights into fungal stress responses and morphological adaptations.

The ascomycete fungus *Zymoseptoria tritici* was the first plant pathogen shown to undergo morphological transitions in response to high temperatures (Lendenmann et al., 2016; Motteram et al., 2011). *Z. tritici* is distributed globally and is the most damaging pathogen in European wheat crops (Torriani et al., 2015). It exhibits a striking morphological variation where different *Z. tritici* strains can present different morphologies in response to the same environmental conditions (Francisco et al., 2019). Four MAPK pathways were identified in this fungal pathogen, including *ZtFus3* (Cousin et al., 2006), *ZtHog1* (Mehrabi et al., 2006b), *ZtSlt2* (Mehrabi et al., 2006a), and cAMP/PKA (Mehrabi et al., 2009; Mehrabi and Kema, 2006), through studies that investigated the role of those MAPK genes in the biology and fitness of this species. However, to date, no comprehensive study has investigated the entire regulatory network of MAPK pathways in response to environmental cues in *Z. tritici*. In most strains, temperatures ranging from 15°C to 18°C induce blastosporulation (blastospore replication by budding – generating a "yeast-like form") while elevated temperatures (from 25°C to 28°C) promote a transition to hyphal growth, pseudohyphae or chlamydospore production (Francisco et al., 2019; Motteram et al., 2011), but some strains do not shift their morphology when placed at different temperatures. The ability to switch among different cell morphologies is critical for the survival of most filamentous fungi, with different types of cells playing different roles during their life cycles. For example, the blastospores of *Z. tritici* can form from germinating pycnidiospores on the surface of wheat leaves and may increase disease transmission during an epidemic (Francisco et al., 2019). Hyphal growth is essential for virulence in *Z. tritici* (Kema et al., 1996); a mutant unable to transition to the hyphal morphology is non-pathogenic (Mehrabi et al., 2006b). Pseudohyphae are distinguished from true hyphae by constrictions formed at the septal junctions, leading to a loss in cytoplasmic continuity between cells (Veses and Gow, 2009). Though little is known about the ecological significance of pseudohyphae, it is suggested that this morphotype facilitates scavenging for nutrients and mobility within the host (Gancedo, 2001; Khang et al., 2010; Thompson et al., 2011). In contrast to pseudohyphae, chlamydospores are spherical thick-walled cells known to allow fungi to persist as resting spores during harsh conditions and to infect host tissues once the environment becomes more conducive to growth (Abou-Gabal and Fagerland, 1980; Couteaudier and Alabouvette, 1990; Francisco et al., 2019). In fact, chlamydospores produced by *Z. tritici* were shown to survive several stresses that killed other cell types (Francisco et al., 2019), although their importance in natural infections remains unknown. All of these morphotypes can be produced during the asexual vegetative growth phase of *Z. tritici* (Francisco et al., 2019), but it remains unclear how the transitions among these modes of growth are regulated. The natural morphological variability observed in pleomorphic fungi is often explained by variation in the genetic background, usually by combining a particular set of alleles that contribute to the phenotype in question. Given the complexity of this trait and the natural variation in morphological responses found within field populations of *Z. tritici* (Francisco et al., 2019), we hypothesized that alleles associated with temperature-related morphotypes could be identified using quantitative trait locus (QTL) mapping.

Here, we report the morphological variability of five global field populations of *Z. tritici* in response to heat stress. We conducted a QTL mapping study using a mapping population derived from parental strains exhibiting contrasting morphological responses. We identified a genomic region responsible for temperature-dependent morphogenesis in *Z. tritici*, and we functionally characterized the genes within this region. Among them, we found that the homolog of Yvh1, a well-known protein phosphatase and here named *ZtYvh1*, is required for hyphal growth. We also found that a transcription factor named *ZtMsr1* functions as a hyphal repressor and a chlamydospore inducer. Though both genes contribute to morphological transitions in *Z. tritici*, *ZtMsr1* plays a major role in the differential heat stress response observed between the parental strains. Finally, we discovered that chlamydospore formation is a response to the intracellular osmotic stress generated during heat stress rather than being a response to the temperature upshift itself. Our experiments elucidate a novel regulatory circuit controlling differential morphotype transitions in a fungal plant pathogen, and illuminate the complex genetic architecture underlying temperature-dependent morphogenesis in pleomorphic fungi.

2. Material and methods

2.1. Fungal isolates and growth conditions

A total of 141 isolates from natural populations and 231 offspring individuals of *Z. tritici* were used to assess the morphological stress response in this fungus (Tables S1 and S2). The two Swiss *Z. tritici* strains ST99CH_1A5 (abbreviated as 1A5) and ST99CH_1E4 (abbreviated as 1E4), and 15 derived mutant lines from these strains were also used here (Fig. S1). The knocked-out IPO323*ΔZtSlt2* (Mehrabi et al., 2006a) and IPO323*ΔZtHog1* (Mehrabi et al., 2006b) mutants were provided by Marc-Henri Lebrun (National Institute of Agricultural Research – INRAE). Because the MAPK mutants were generated in the genetic background of IPO323 (Kema and van Silfhout, 1997), this strain was also used as a control. Fungal cells were routinely retrieved from glycerol at −80°C and grown on YSB (10 g/L yeast extract, 10 g/L sucrose, and 50 μg/mL kanamycin sulfate; pH 6.8) medium at 18°C for four days. Cell concentrations were determined by counting blastospores using the KOVA cell chamber system (KOVA International Inc., USA) and kept on ice until required for the phenotypic assays.

2.2. Phenotyping for the temperature-dependent morphotypes

Blastospore suspensions of each tested isolate were added to a final concentration of 10^5 blastospores/mL on YSB and incubated at 27°C. After 72 h of incubation, an aliquot was taken and checked by light microscopy using a Leica DM2500 microscope with LAS version 4.6.0 software. Isolates were scored for their stress response to grow as chlamydospores (score = 0), hyphae (score = 1), or as a mixture of chlamydospores and hyphae (score = 2) under the heat stress (Tables S1 and S2).

To determine the global distribution of morphological stress responses, we analyzed 141 isolates of *Z. tritici* collected from single wheat fields between 1990 and 2001 in four distinct locations: Australia, Israel, Switzerland, and Oregon (USA) (Zhan et al., 2005). In Oregon, the isolates were sampled from the resistant cultivar Madsen (Oregon R) and the susceptible cultivar Stephens (Oregon S).

To analyze the genetic architecture of temperature-dependent morphogenesis, we used a *Z. tritici* mapping progeny population consisting of 231 offspring individuals from the cross between 1A5 and 1E4 (Lendenmann et al., 2014). These two parental strains were sampled from the same naturally infected wheat field in Switzerland in 1999 (Zhan et al., 2002) and differ for several traits, including their morphological stress response (Francisco et al., 2019). For instance, 1A5 produces only chlamydospores and 1E4 undergoes mainly filamentation in response to heat stress.

2.3. Genotype data and QTL mapping

For mapping the locus of temperature-dependent morphogenesis, we used the genetic map generated by Zhong et al. (Zhong et al., 2017). SNP data of 261 offspring isolates from the cross between 1A5 and 1E4 were obtained from RAD sequencing data (Lendenmann et al., 2014), but using the finished genome of the 1A5 strain (Plissonneau et al., 2018) as the reference genome for the cross. SNP markers were generated and filtered as described in a previous study (Zhong et al., 2017). This provided 35′030 SNP markers in the 1A5 × 1E4 cross with an average marker distance of 1′145 bp (equivalent to 0.31 cM). The QTL analysis was based on the phenotypic score given to each offspring isolate, as demonstrated in Tables S2 and S3. The Single-QTL genome scan using the standard interval mapping (SIM) was performed in the R/qtl package (Arends et al., 2010) to improve the marker regression method by estimating pseudomarkers between true markers. The significance thresholds of logarithm of odds (LOD) of the QTLs were based on 1000 permutation tests across the entire genome, followed by Bayesian credible intervals used to calculate 95% confidence intervals of the QTL. Genes within the 95% confidence interval were identified according to the genome annotations of the reference parental strains (Plissonneau et al., 2018).

2.4. Identification of candidate genes within the QTL confidence interval

All genes within the QTL confidence interval had their genomic sequences compared to identify allelic variants among the genome sequences of the two parental strains using AliView software (Larsson, 2014). We evaluated genes for the presence of non-synonymous SNPs and other sequence variation either in the protein-encoding sequence or the 5′- or 3′-UTR. To define the length of UTR regions, we used the *in planta* and *in vitro* expression data of the 1A5 and 1E4 parental strains obtained from previous studies (Francisco et al., 2019; Palma-Guerrero et al., 2017). The candidate genes were BLASTed to the NCBI database (https://blast.ncbi.nlm.nih.gov/Blast.cgi) to confirm their functional domains and to search for orthologs in other fungal species. Synteny of the 1A5 and 1E4 genome sequences in the QTL region was analyzed using pairwise blastn on repeat-masked genomic sequences and visualized using the genoPlotR package in R (Guy et al., 2010).

2.5. Ortholog identification, protein alignment and phylogenetic analysis

The protein sequences of the candidate genes were used for a Blastp analysis against the NCBI database (National Center of Biotechnology Information). A dataset containing their counterpart proteins were used for phylogenetic analysis. Protein sequences were aligned using the AliView program (Larsson, 2014). The best-fit model of amino acid evolution was the LG + G, determined by MegaX software (Stecher et al., 2020). Amino acid sequences were aligned using Muscle followed by maximum likelihood phylogeny reconstruction using 1,000 bootstraps and performed with the software MegaX (Stecher et al., 2020).

2.6. Plasmid constructions and transformations

DNA assemblies were conducted with the In-Fusion HD Cloning Kit (Takara BIO) following the manufacturer's instructions. A summary of the plasmids and their constructions is given in Fig. S1 and primers used in this study are listed in Table S4. To create the construct for ectopic integration of *ZtMsr1*$_{1A5}$ into the 1E4 genetic background, a fragment containing *ZtMsr1*$_{1A5}$, 1 Kb upstream of the start codon, and 1 Kb downstream of the stop codon were amplified from 1A5 genomic DNA. The pES1 plasmid (obtained from E. H. Stukenbrock, Kiel University, unpublished) carrying the hygromycin resistance cassette and used as a selectable marker was linearized with *Xba*I and *Him*III (New England Biolabs). The two fragments were assembled into pES1 resulting in pES1-Ect$_{ZtMsr1\text{-}1A5}$. To knock-out the genes *Zt11059*, *ZtYvh1*, or *ZtPtc5* in the 1E4 strain, 1 Kb of both flanking regions for each gene were amplified from the 1E4 genomic DNA. The pES1 plasmid was digested with *Kpn*I and *Sbf*I (New England Biolabs) for plasmid linearization, and three fragments of each construct were assembled into pES1 carrying the hygromycin resistance cassette and used as selectable marker, resulting in pES1-1E4Δ*Zt11059*, pES1-1E4Δ*ZtYvh1*, and pES1-1E4Δ*ZtPtc5*. The *ZtMsr1* and *ZtYvh1* genes were also knocked-out in the 1A5 strain. The pES1 plasmid linearized with *Kpn*I and *Sbf*I (New England Biolabs) and the two flanking regions of each gene were assembled into pES1, resulting in pES1-1A5Δ*ZtMsr1* and pES1-1A5Δ*ZtYvh1*. To create the constructs for ectopic integration of the *ZtYvh1*$_{1E4}$ or *ZtYvh1*$_{1A5}$ genes into the 1E4Δ*ZtYvh1* mutant strain, the pCGEN plasmid carrying the geneticin resistance cassette as a selective marker (Motteram et al., 2011) was linearized with *Kpn*I (New England Biolabs). A fragment containing the *ZtYvh1*$_{1E4}$ or *ZtYvh1*$_{1A5}$ genes and 1 Kb of their respective flanking regions were amplified from 1E4 or 1A5 genomic DNAs, respectively, and cloned into pCGEN, resulting in pCGEN-1E4-Ect$_{ZtYvh1\text{-}1E4}$ or pCGEN-1E4-Ect$_{ZtYvh1\text{-}1A5}$. *Z. tritici* cells were transformed via *Agrobacterium*-mediated transformation according to the protocol adapted by Meile et al., 2018 (Meile et al., 2018). We confirmed the mutant lines by a PCR-based approach using a forward primer specific to the upstream sequence of the inserted cassette and a reverse primer specific to the selective gene. We determined the copy number of the transgene by quantitative PCR (qPCR) on genomic DNA extracted with the DNeasy Plant Mini Kit (Qiagen). Lines with a single insertion were selected for further experiments.

2.7. Phenotypic characterization of the mutants

Blastospore suspensions of each strain were inoculated into three flasks containing YSB at a final concentration of 10^5 blastospores/mL and incubated at 18°C (as control) or 27°C for three days. The cell morphology was observed by light microscopy every 24 h after incubation (hai) until 72 hai. We used the morphology of the 1A5 or 1E4 strains as references.

To test for altered vegetative growth, we used water agar (WA – 12 g/L agar, and 50 μg/mL kanamycin sulfate) medium to induce hyphal growth. 200 μL of a blastospore suspension of each tested strain was plated at a final concentration of $2x10^2$ blastospores/mL on five independent WA plates and incubated in the dark at 18°C for 15 days post-inoculation (dpi). Because mycelial growth on WA plates exhibited poor color contrast, the colony diameters were measured manually. All measurements included at least 20 colonies. The colony diameter values were divided by two to generate the radial growth (mm) values, which were plotted in a violin plot ggplot2 package from R (Wickham, 2009). Analysis of variance (ANOVA) was performed using the agricolae package (Mendiburu, 2015). The radial growth (mm) of 1A5 and 1E4 strains was used to calculate the percentage of growth inhibition (% reduction in growth radius) of each mutant. A *t*-test statistic was used to test the hypothesis that mutants were affected in their vegetative growth compared to the wild-type strains.

To assess the contribution of the candidate genes to the cell wall integrity, we exposed blastospores of the tested strains to different stress conditions, including oxidative stress (1 mM of hydrogen peroxide – H_2O_2), osmotic stress (1 M sorbitol), cell wall stress (2 mg/mL Congo red), and plasma membrane stress (0.01% sodium dodecyl sulfate).

Blastospore suspensions of each strain were serially diluted to $4x10^7$, $4x10^6$, $4x10^5$, and $4x10^4$ blastospores/mL and drops of 3.5 μL were plated onto five independent potato dextrose agar plates (39 g/L potato dextrose agar, and 50 μg/mL kanamycin sulfate) amended with the above-mentioned stresses, and incubated at 18°C in a dark room. Blastospore suspensions plated only onto PDA plates were used as a control. After incubation, the fungal colonies were visually scored for a binary phenotype (i.e., growth or inhibition) based on digital images taken at 6 dpi.

2.8. Osmoregulation assay

Blastospore suspensions of the mutant lines and their respective wild-type strains were inoculated onto YSB medium amended with 1 M sorbitol at a final concentration of 10^5 blastospores/mL and incubated at 27°C. Flasks containing only YSB medium were used as controls. An aliquot was taken from each flask at 24, 48, and 72 hai to monitor cell morphology by light microscopy.

2.9. The use of MAPK mutants as proof of concept

To evaluate the role of the MAPK CWI and HOG pathways in thermotolerance (Dunayevich et al., 2018; Fuchs and Mylonakis, 2009; Winkler et al., 2002), we tested whether these two MAPK pathways also play a role in the temperature-dependent morphogenesis described here using IPO323ΔZtSlt2 and IPO323ΔZtHog1 mutants, as proof of concept. Blastospore suspensions of each strain were inoculated onto YSB at a final concentration of 10^5 blastospores/mL and incubated at 18°C (as control) or 27°C. The 1A5, 1E4 and IPO323 *Z. tritici* strains were used as references. Cell morphologies were analyzed by light at 24, 48, and 72 hai. Cells harvested at 72 hai were also fixed with 70% (v/v) ethanol for 30 min, followed by three washes with phosphate-buffered saline (PBS). The cells were stained with 1 μg/mL of the chitin-binding dye Calcofluor white (CFW) (Sigma-Aldrich Chemie Gmbh, Munich, Germany) for 15 min. The stained cells were viewed with a Leica DM2500 fluorescence microscope using a UV filter system for CFW consisting of a BP excitation filter at 340–380 nm and a long pass emission filter (>425 mm).

3. Results

3.1. The global distribution and genetic architecture of temperature-dependent morphotypes

We previously reported that two field isolates of *Z. tritici* differ in their production of chlamydospores under heat stress (Francisco et al., 2019). Here, we expand upon this finding by assessing the morphological responses of 141 *Z. tritici* isolates from five worldwide field populations under heat stress (27°C) (Table S1 and Fig. 1). In four out of five populations the majority of the isolates exhibit hyphal growth, but in the Israeli population, 77% (n = 23) of the isolates switched to chlamydospores at high temperatures. 10% (n = 14) of the worldwide isolates grew as a mixture of hyphae and chlamydospores (Fig. 1A). We assume that the global populations have evolved under different environmental conditions and that local adaptations in each population may have resulted in distinct genetic elements and regulatory pathways that contribute to the mixture of temperature-dependent morphotypes found in each field. Regardless of their geographical origin, chlamydospore- or hyphal-forming isolates shared the same morphological features (Fig. 1B-C), including the spherical and thickened cell walls characteristic of chlamydospores and the elongated cell walls lacking constrictions in hyphae (Whiteway and Bachewich, 2007).

To analyze the genetic architecture of temperature-dependent morphogenesis, the segregating F1 population from a cross between strains 1A5 and 1E4 were scored for its morphological response to grow as hyphae, chlamydospores, or both morphotypes at 27°C. The observed morphotype for each offspring is given in Table S2 and summarized in Fig. 2B, and their associated frequencies are described in Fig. 2C. A genome scan of the F1 population identified a single QTL on chromosome 12 with a logarithm of odds (LOD) score of 17.8 (Fig. 2A and D). The QTL confidence interval was determined by the pseudomarkers at chr12.loc322 (LOD = 17.3), chr12.loc325 (LOD = 17.8), and chr12.loc329 (LOD = 16.8), which were flanked by the true SNP markers 12_1226988 (chr12.loc316) on the left and 12_1258185 (chr12.loc334) on the right side of the QTL (Fig. 2F). The 12_1226988 and 12_1258185 markers were used to model the allele effects. We found that the flanking 1E4 parent alleles provided a higher phenotypic mean (60% and 57% higher, respectively) than the flanking 1A5 parent alleles (Fig. 2E). The chromosome 12 QTL identified a 95% confidence interval of 31 Kb containing only eight genes (Fig. 2G and Table S5). Only ~ 25% of the variation in phenotypes was explained by the chromosome 12 QTL and the phenotypic distribution patterns in the progeny population displayed a non-Mendelian segregation ratio (Fig. 2C). Taken together, these results suggest that temperature-dependent morphogenesis is a complex trait controlled by a number of genetic and environmental factors, i.e. it is a quantitative trait that is not inherited in a simple Mendelian fashion (Falconer, 1996).

3.2. Four candidate genes were identified within the QTL confidence interval

Among these genes, we focused on those predicted to encode a gene function related to cell development and containing at least one sequence variant between the 1A5 and 1E4 alleles either in 5′ or 3′ UTRs or in the protein-encoding sequence by displaying nonsynonymous amino acid substitutions (Table S5). The four genes meeting these criteria were *1A5.g11037, 1A5.g11038*, and *1A5.g11039* exhibiting sequence polymorphism between the parental strains, while *1A5.g11034* is disrupted by a hAT transposon in the 1E4 strain (Table S5 and Fig. S2). Two of the genes encoded putative transcription factors (TFs) that we named *ZtMsr1* (*morphological stress response 1*) (*1A5.g11034*) and *Zt11037* (*1A5.g11037*). *ZtMsr1* and *Zt11037* encode proteins containing GAL4-like $Zn(II)_2Cys6$ and C2H2 zinc finger domains, respectively, but orthologs have not yet been characterized. The other two genes encoded protein phosphatases named ZtYvh1 (*1A5.g11038*) and ZtPtc5 (*1A5.g11039*). ZtYvh1 is orthologous to the dual-specificity protein phosphatase Yvh1 that was first identified as a yeast vaccinia virus VH1 phosphatase in *Saccharomyces cerevisiae* (Guan et al., 1992), and has since been characterized in other fungi (Beeser and Cooper, 2000; Hanaoka et al., 2005; Yin et al., 2016). ZtPtc5 is orthologous to Ptc5 of *S. cerevisiae,* a protein located in the mitochondrial compartment (Gey et al., 2008; Krause-Buchholz et al., 2006). A list of orthologs and their phylogenetic relationships are summarized Fig. S3.

3.3. The transcription factor ZtMsr1 functions as a hyphal repressor and activator of chlamydospore production, while the protein phosphatase ZtYvh1 is required for fungal filamentation

Next, we generated mutant lines for the *ZtMsr1*, *Zt11037, ZtYvh1,* and *ZtPtc5* genes (Fig. S1) and tested their response to heat stress (27°C) (Figs. 3, 4, and S3). Blastospores from 1E4 switched to hyphal growth, while 1A5 produced swollen cells and mature chlamydospores at 48 and 72 h after incubation (hai), respectively. The ectopic insertion of the 1A5 *ZtMsr1* allele into 1E4, a strain with *ZtMsr1* disrupted by a TE, induced chlamydospore formation (Fig. 3A). At 24 hai, the 1E4-$Ect_{ZtMsr1\text{-}1A5}$ mutants displayed a reduction in filamentation and hyphal branches, and an increase in chlamydospore formation, a phenotype that was also observed at later time points. Similarly, deleting the functional *ZtMsr1* in 1A5 resulted in a switch to hyphal growth at 24 hai. Hence, *ZtMsr1* appears to function as a repressor of hyphal growth and activator of chlamydospore production during heat stress (Fig. 3A).

We found that the deletion of *ZtYvh1* drastically reduced filamentation in 1E4 and induced formation of pseudohyphae and

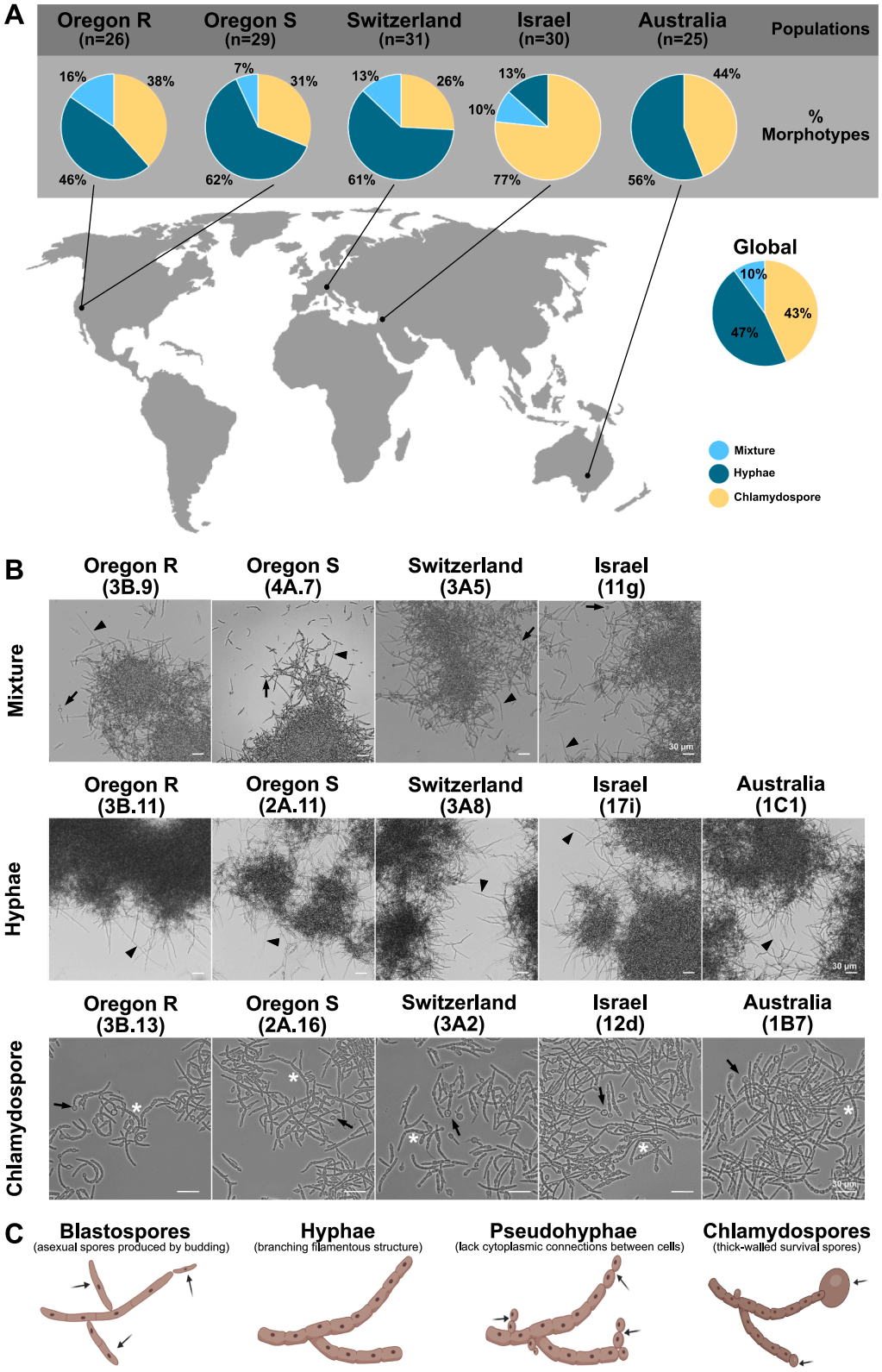

FIG. 1. Global field populations of *Zymoseptoria tritici* vary in their heat stress response. (A) Sampling locations and the associated frequencies of isolates growing as chlamydospores or hyphae upon exposure to elevated temperature (27°C). Individuals that exhibited both morphotypes at high temperatures were termed mixtures. Oregon R and Oregon S correspond to strains obtained from the resistant cultivar Madsen and the susceptible cultivar Stephens, respectively. (B) Micrographs of typical morphotypes of mixture- (upper panel), hyphal- (middle panel), or chlamydospore-growing isolates (lower panel) of each population. Black triangles indicate hyphae growth, white asterisks point to pseudohyphae, and black arrows demonstrate the chlamydospore cells. (C) Illustrations of the four morphotypes produced during vegetative growth of *Z. tritici*, such as blastospores, hyphae, pseudohyphae, and chlamydospores. Image created with BioRender.com.

chlamydospores at 24 and 48 hai, respectively; however, the morphological response of the 1A5Δ*ZtYvh1* null mutant did not differ from its 1A5 wild-type (Fig. 4A). This led us to hypothesize that the 1A5 strain may carry a non-functional allele of *ZtYvh1*. To test this hypothesis, we complemented the 1E4Δ*ZtYvh1* with either the 1E4- or 1A5-*ZtYvh1* alleles. Hyphal growth was restored in both 1E4Δ*ZtYvh1* + $Ect_{ZtYvh1\text{-}1E4}$ and 1E4Δ*ZtYvh1* + $Ect_{ZtYvh1\text{-}1A5}$ mutants (Fig. 4A), demonstrating that, despite the high sequence polymorphism exhibited by the parental strains, both *ZtYvh1* alleles appear to be functional. We conclude that Yvh1 is involved in the blastospore-to-hyphae transition in *Z. tritici*, but is not responsible for the differential heat stress responses between the parental strains. Finally, no altered phenotypes were observed for

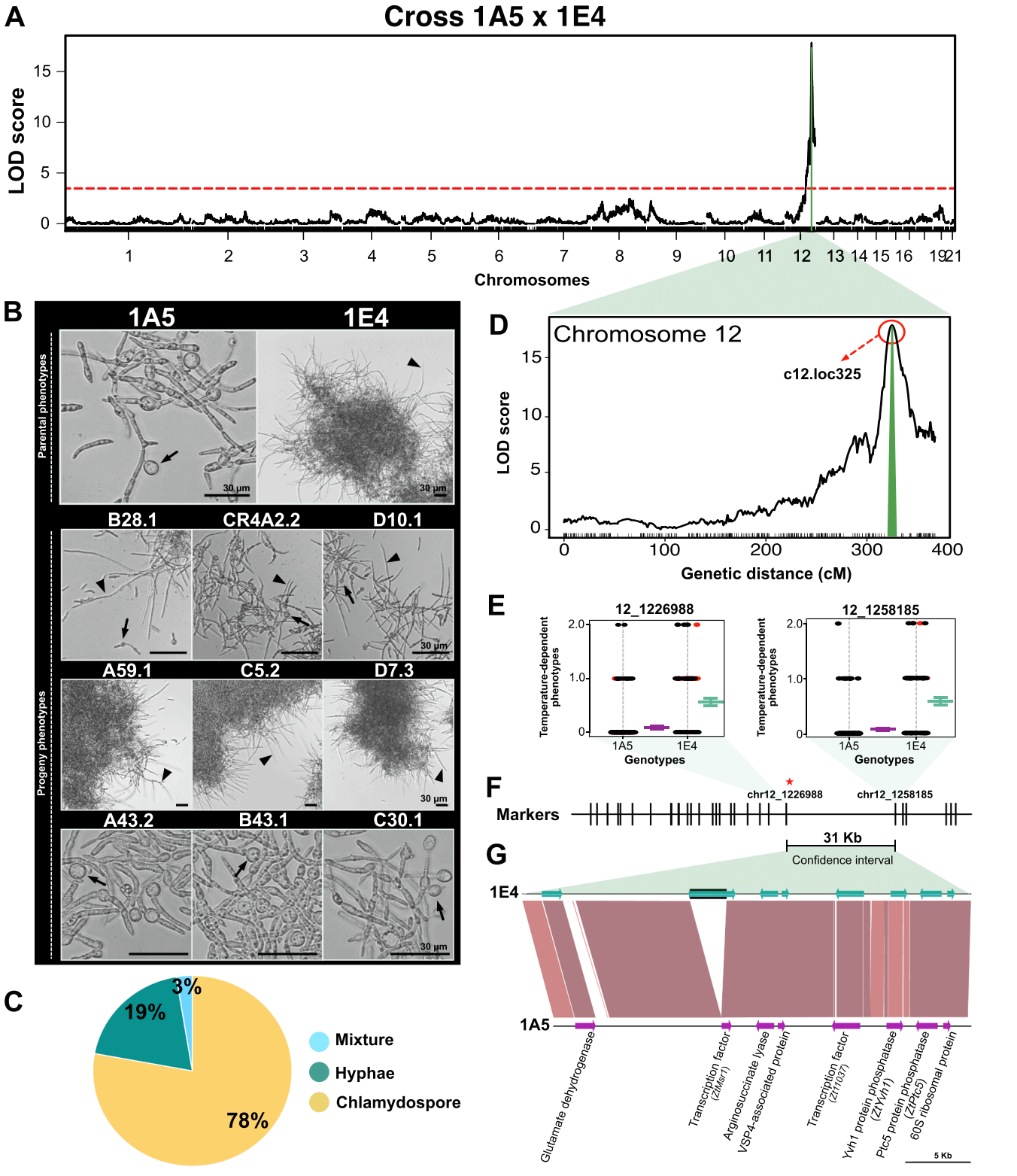

(caption on next page)

FIG. 2. A QTL on chromosome 12 is correlated to temperature-dependent morphogenesis. (A) Interval mapping for the 1A5 (morphotype chlamydospore) × 1E4 (morphotype hyphal) cross. The y-axis shows the $\log_{10}$ of the odds (LOD score) values, and the x-axis indicates the chromosome numbers. The dashed horizontal red line represents the significance threshold ($p = 0.05$). (B) Representation of the morphological responses displayed by the parental strains and individuals from the segregating F1 population. The 1A5 parental strain produces chlamydospores (black arrow) without any evidence of hyphal differentiation, while 1E4 undergoes mainly filamentation in response to heat stress. Below the micrographs are shown the typical morphotypes of mixture- (upper panel), hyphal- (middle panel), or chlamydospore-growing isolates (lower panel) exhibited by the progeny. Black triangles indicate hyphae growth and black arrows demonstrate the chlamydospore cells. (C) The associated frequencies of isolates growing as hyphae, chlamydospores or a mixture of both morphotypes upon exposure to elevated temperature at 27°C. (D) LOD plot of the chromosome 12 QTL. The x-axis indicates the genetic distances (centimorgans - cM) along chromosome 12. The detected QTL has the highest LOD at 325 cM and the 95% confidence interval is indicated by a green color. (E) Allele effects corresponding to the QTL shown in (D). Numbers on the top of each plot are SNP markers with the highest LOD in the QTL and delimit the confidence interval. Each circle represents a different offspring. A red circle indicates that the genotype at the locus was missing and was inferred based on single imputations. (F) SNP markers surrounding the confidence interval are shown as vertical lines. The 12_1226988 marker on the left and the 12_1258185 marker on the right delimited the 31 kilobase (Kb) confidence interval of the QTL. A red star indicates the true SNP marker (12_1226988) closest to the pseudomarker chr12.loc325 (LOD = 17.83) with the highest LOD score. (G) Synteny plot showing the genes located within the chromosome 12 QTL and DNA polymorphism in this genomic region. The darker the red color, the lower the degree of polymorphism between 1A5 and 1E4 parental strains. The arrows represent the genes and the black square indicates a transposable element. (For interpretation of the references to color in this figure legend, the reader is referred to the web version of this article.)

1E4Δ*Zt11037* and 1E4Δ*ZtPtc5* compared to its 1E4 wild-type (Fig. S4), therefore no further analyses were performed for these mutants.

3.4. *ZtMsr1 and ZtYvh1 contribute to vegetative growth and cellular integrity*

Because some mutants displayed altered filamentation, we hypothesized that *ZtMsr1* and *ZtYvh1* may also contribute to the mycelial growth phase of *Z. tritici*. To test this hypothesis, we compared the growth of the mutants with their respective wild-types grown on water agar (WA) medium - a nutrient-poor environment that induces hyphal growth (Fig. 3B-C and 4B-C). The vegetative growth inhibition for each tested strain is shown in Table S6 and summarized in Table S7. The 1E4-Ect$_{ZtMsr1\text{-}1A5}$ mutants showed a growth inhibition of 70% (Fig. 3B and Table S6) and a derepressed blastosporulation on WA compared to the 1E4 wild-type (Fig. 3C). In contrast, deletion of *ZtMsr1* in the 1A5 strain did not affect colony sizes in the nutrient-poor WA environment (Fig. 3B). Although the growth kinetics did not appear to be affected, the 1A5Δ*ZtMsr1* produced compact hyperfilamented colonies with repressed blastospore formation (Fig. 3C), a phenotype regularly observed in the 1E4 colonies. This finding confirms that *ZtMsr1* acts as a transcriptional repressor of hyphal growth in *Z. tritici*.

Deletion of *ZtYvh1* significantly impacted vegetative growth of *Z. tritici* independently of the genetic background (Fig. 4B-C). The radial growth of 1E4Δ*ZtYvh1* colonies was reduced by 75% compared to 1E4 wild-type on WA plates, while 1A5Δ*ZtYvh1* growth was diminished by 82% compared to the 1A5 wild-type strain (Fig. 4B and Table S6). The *ZtYvh1* deletion derepressed blastospore formation in nutrient-poor medium, and colonies of 1E4Δ*ZtYvh1* or 1A5Δ*ZtYvh1* mutants showed extensive blastosporulation on WA, especially in the innermost part of the colony (Fig. 4C). Nevertheless, the fungal growth suppression observed for the 1E4Δ*ZtYvh1* mutant was restored in the 1E4Δ*ZtYvh1* + Ect$_{ZtYvh1\text{-}1E4}$ and 1E4Δ*ZtYvh1* + Ect$_{ZtYvh1\text{-}1A5}$ allele swap mutants (Fig. 4C and Table S6), corroborating that *ZtYvh1* is required for hyphal growth in *Z. tritici*.

Because regulatory circuits controlling heat stress responses are also known to affect cell wall synthesis (Chow et al., 2018; Fuchs and Mylonakis, 2009), we next asked if *ZtMsr1* and *ZtYvh1* are also involved in maintaining the cellular integrity of *Z. tritici*. We exposed all tested strains to four different cell wall and membrane stressors (Fig. S5A and Table S7). Deletion of *ZtMsr1* or *ZtYvh1* did not affect the tolerance of *Z. tritici* to hyperosmotic or oxidative stresses caused by sorbitol or H_2O_2, respectively (Fig. S5A). Also, the presence/absence of *ZtMsr1* did not influence fungal growth on potato dextrose agar (PDA) supplemented with SDS, a compound that causes alterations in cell membrane permeability and induces intracellular oxidative stress (Cao et al., 2020). In contrast, the presence of *ZtMsr1* does play a crucial role in cell wall sensitivity. The ectopic integration of the 1A5 *ZtMsr1* allele into the 1E4 strain strongly inhibited fungal growth on PDA supplemented with Congo Red (CR), which inhibits fungal cell wall assembly by binding to chitin and β-1,3 glucan (Kopecká and Gabriel, 1992). Interestingly, the 1A5Δ*ZtMsr1* null mutant showed substantial tolerance to CR (Fig. S5A). These findings suggest that the presence of *ZtMsr1* increases perception of cell wall stresses which may prevent the fungus from growing under harmful conditions.

In line with previous studies (Liu et al., 2016; Sacristan-Reviriego et al., 2015), the *ZtYvh1* mutants displayed hypersensitivity to cell-wall perturbing compounds (Fig. S5A). The 1A5Δ*ZtYvh1* growth was significantly inhibited on PDA supplemented with CR, while 1E4Δ*ZtYvh1* could not grow in the presence of this compound. Both the 1E4Δ*ZtYvh1* and 1A5Δ*ZtYvh1* mutants showed a reduced tolerance to SDS (Fig. S5A). The reconstitution of 1E4Δ*ZtYvh1* by the wild-type *ZtYvh1* alleles of either 1E4 or 1A5 restored its growth defect on both CR and SDS (Fig. S5B), confirming that both alleles are functional and that Yvh1 plays a role in fungal cell wall integrity.

3.5. *Deletion of protein kinases from the CWI and HOG pathways result in chlamydospore formation*

Due to the role of the MAPK CWI and HOG pathways in thermotolerance and cell wall synthesis in fungi (Dunayevich et al., 2018; Fuchs and Mylonakis, 2009; Winkler et al., 2002), we asked if these two pathways also mediate filamentous growth or chlamydospore production in *Z. tritici* during heat stress. As proof of concept, we tested the previously available IPO323Δ*ZtSlt2* and IPO323Δ*ZtHog1* MAPK mutants and its wild-type IPO323 strain for their morphological response at 27°C (Fig. S6A). High temperature induced swollen cells and chlamydospore-like structures at 24 hai and 72 hai, respectively, in both IPO323Δ*ZtSlt2* and IPO323Δ*ZtHog1* mutants. Their morphological responses resembled 1A5, but differed from 1E4 or IPO323 that showed only hyphal growth. Chlamydospores are thick-walled structures that show chitin accumulation in the cell wall (Francisco et al., 2019). To measure this property, we stained the putative chlamydospore cells with the chitin-binding dye Calcofluor white (CFW). Chitin accumulation was noticeable only in the septa of the suspensor cells (the distal part of differentiated hyphae where chlamydospores are formed) or hyphae in the 1E4 and IPO323 strains, whereas the cell wall of the chlamydospore-like cells was highly stained by CFW in IPO323Δ*ZtSlt2* and IPO323Δ*ZtHog1,* as observed for chlamydospores produced by the 1A5 strain (Fig. S6A), confirming that they were true chlamydospores.

3.6. *Chlamydospore formation is a response to the intracellular osmotic stress generated by the heat stress*

When exposed to thermal stress, fungal cells rapidly accumulate trehalose to prevent protein denaturation, creating an intracellular hyperosmotic condition and turgor pressure (Mensonides et al., 2005; Singer and Lindquist, 1998; Zhao et al., 2018), which induces the efflux

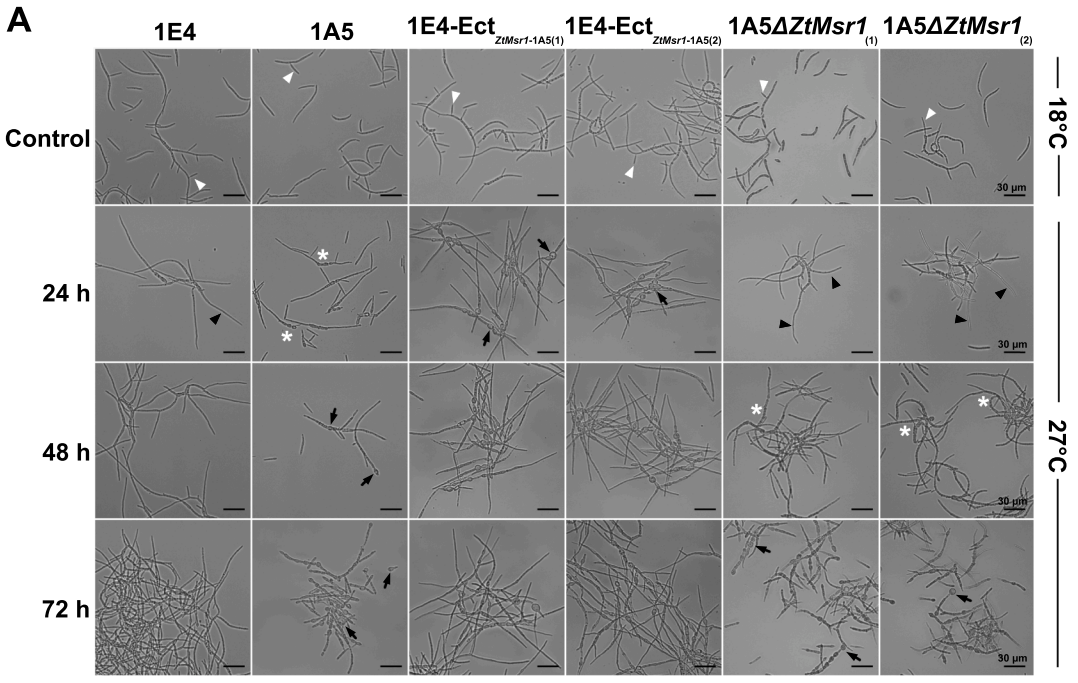

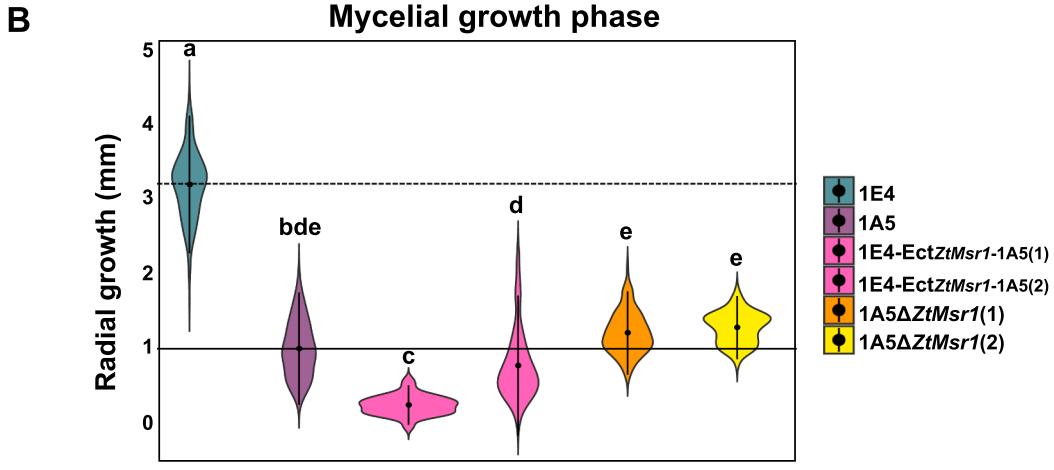

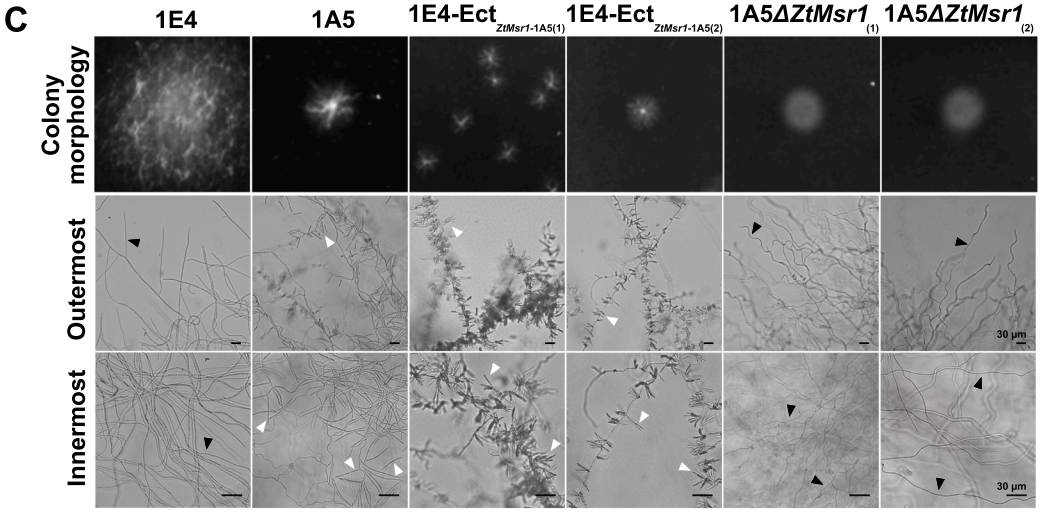

(caption on next page)

FIG. 3. *ZtMsr1* plays a major role in the differential heat stress response observed between the parental strains. (A) Blastospores incubated on nutrient-rich YSB medium at 18°C (control environment) multiply by budding as blastospores (white triangles). The effect of heat stress on *Z. tritici* morphology was observed by exposing the strains at 27°C for 72 h. The 1E4 strain responds to a high temperature by switching mainly to filamentous growth (black triangles), while 1A5 produces pseudohyphae (white asterisks) and chlamydospores (black arrows) as heat stress responses. The 1E4-Ect$_{ZtMsr1\text{-}1A5}$ mutants produced chlamydospores (black arrows) after 24 h, while the deletion of *ZtMsr1* in the 1A5 strain derepressed filamentation (black triangles). All experiments were conducted independently three times with similar results. Numbers within brackets represent independent mutant lines. (B) Blastospores incubated on nutrient-limited WA at 18°C switch to hyphal growth. Violin plots demonstrate the radial growth (mm) of at least 20 colonies of each tested strain. The ectopic integration of 1A5-*ZtMsr1* into 1E4 produced smaller colonies compared to 1E4 wild-type, but the deletion of *ZtMsr1* in 1A5 did not affect colony size. The dashed or solid horizontal lines indicate the median of the radial growth (mm) of 1E4 and 1A5 strains, respectively. Different letters on the top of the bars indicate a significant difference among the tested strains according to Analysis of Variance (ANOVA). All experiments were conducted independently three times with similar results. (C) Overview images of colony morphology and light microscopies of the outermost and innermost regions of the colonies described in (B). Colonies from 1E4-Ect$_{ZtMsr1\text{-}1A5}$ mutants showed extensive blastosporulation resembling the 1A5 strain. On the other hand, 1A5Δ*ZtMsr1* colonies were hyperfilamented similar to 1E4. Black triangles point to hyphae and white triangles demonstrate areas of blastospore formation.

and influx of cellular osmolytes in a feedback system (Hohmann, 2002) governed by cross-talk between the CWI and HOG pathways (Dunayevich et al., 2018; Rodriguez-Pena et al., 2010). We hypothesized that chlamydospore formation is a consequence of a differential fungal perception and/or a response to the changing intracellular osmotic environment during heat stress. To test these hypotheses, we inoculated the 1A5, 1E4, and IPO323 strains and their derived mutants on YSB medium amended with 1 M sorbitol, used as an osmotic stabilizer, and incubated at 27°C (Figs. 5 and S6B). We found that 1E4 and IPO323 maintained their hyphal growth response, independently of the osmotic condition. In contrast, 1A5 and the *ZtMsr1*, *ZtYvh1*, IPO323Δ*ZtSlt2,* and IPO323Δ*ZtHog1* mutants that were previously found to undergo chlamydospore formation as the bona-fide heat stress response, switched to filamentous growth in this osmotic stabilized environment (Figs. 5 and S6B), except for IPO323Δ*ZtHog1* which recovered its yeast-like growth (Mehrabi et al., 2006b) (Fig. S6B). Thus, we concluded that the differential perception of the intracellular osmolarity and turgor pressure function as a crucial signal that determines the regulatory cascade controlling the morphogenic responses under heat stress.

4. Discussion

Global warming is likely to have a significant effect on fungal populations, favoring thermotolerant strains or those producing heat-resistant survival structures. This study extends previous observations on temperature-dependent morphogenesis in fungi (Nichols et al., 2007; Shapiro and Cowen, 2012; Wang and Lin, 2012). Previously, we showed that Swiss *Z. tritici* strains produce chlamydospores as a temperature-dependent morphotype (Francisco et al., 2019). Here, we demonstrated that *Z. tritici* populations from around the world can grow as hyphae or chlamydospores in response to heat stress. The different cellular morphologies observed in field populations of *Z. tritici* from around the world, including blastospores, hyphae, and chlamydospores, may affect the fitness of *Z. tritici* strains at different points in their life cycle, with the ability to switch among morphologies governed by natural genetic variations. We showed that these variations can affect the flexibility and survival of a fungal population facing environmental changes (Francisco et al., 2019). These findings motivated us to investigate the genetic basis of temperature-dependent morphogenesis in this fungus. Using QTL analysis, we identified genes regulating morphogenic transitions in *Z. tritici.* Our data proposes a complex mechanism underlying morphogenic transitions in response to temperature stress (Fig. 6).

We identified a single QTL on chromosome 12 containing only eight genes that explained 25% of the overall variation for a temperature-dependent morphological switch. This illustrates that morphological changes can be inherited as quantitative traits in *Z. tritici* (Lendenmann et al., 2016). Two genes in this QTL, a novel transcription factor named *ZtMsr1* and a protein phosphatase named *ZtYvh1,* regulate the blastospore-to-hyphae/chlamydospore transition in response to heat stress in *Z. tritici.* Zinc cluster transcription factors (TFs) like *ZtMsr1* are key players in the signal transduction pathways regulating a plethora of cellular and stress responses in fungi (Lu et al., 2014; MacPherson et al., 2006). In this study, the deletion of *ZtMsr1* in the 1A5 strain activated hyphal growth, whereas the insertion of the 1A5-*ZtMsr1* allele into the 1E4 strain (in which *ZtMsr1* is naturally disrupted by a TE), induced chlamydospore formation at 27°C. Furthermore, after incubation in a mycelial-inducing environment, the 1E4-Ect$_{ZtMsr1\text{-}1A5}$ mutants showed impaired hyphal growth and derepressed blastosporulation like 1A5, while 1A5Δ*ZtMsr1* mutants exhibited hyperfilamented colonies similar to 1E4. Taken together, our findings indicate that the presence of *ZtMsr1* positively induces chlamydospore formation and hyphal repression in *Z. tritici*. Until now, *Zt107320* was the only zinc cluster TF described to regulate the blastospore-to-hyphae transition in *Z. tritici*; however, that response was to different sources of carbon (Habig et al., 2020). Similar to other dimorphic fungi, the zinc cluster proteins may act as activators, repressors, or as both activators and repressors for specific genes. For example, *Stb5* acts as an activator and a repressor in the budding yeast *Saccharomyces cerevisiae* in response to oxidative stress (Larochelle et al., 2006). The complete repression of hyphal growth or the sole induction of chlamydospore formation in *ZtMsr1* mutants likely depends on contributions from other genetic modifiers, consistent with the polygenic nature of morphological transitions in fungi. Additional studies will be needed to identify *ZtMsr1*-regulated genes and determine if *ZtMsr1* can be self-regulated or regulate other genes within the chromosome 12 QTL.

In contrast to *ZtMsr1,* the protein phosphatase *ZtYvh1* orthologs are well-characterized in eukaryotes. Deletion of *Yvh1* in different fungi causes defects for a multitude of fungal development processes, including vegetative growth and cellular integrity (Beeser and Cooper, 2000; Guan et al., 1992; Hanaoka et al., 2005; Liu et al., 2016; Sacristan-Reviriego et al., 2015). Nevertheless, this is the first time that an *Yvh1* ortholog has been shown to regulate a morphological stress response. Deletion of the 1E4 *ZtYvh1* allele significantly repressed filamentation and induced chlamydospore formation during heat stress, whereas deletion of *ZtYvh1* did not affect the morphological responses of 1A5. At first, this result suggested that the 1A5 *ZtYvh1* phosphatase was not functional. However, the reconstitution of the 1E4Δ*ZtYvh1* mutant with either the 1E4- or 1A5-*ZtYvh1* alleles restored the WT filamentation phenotype and abolished chlamydospore formation upon heat stress, demonstrating that ZtYvh1 is involved in the dimorphic switch, but is not responsible for the differential heat stress responses between the parental strains. Consistent with the pleiotropic role of this phosphatase, the deletion of *ZtYvh1* also affected the vegetative growth of *Z. tritici,* independently of the genetic background. Since the deletion of *ZtYvh1* orthologs in *C. albicans CaYvh1*, *S. cerevisiae ScYvh1*, and *M. oryzae MoYvh1* also cause defects in fungal growth (Beeser and Cooper, 1999; Beeser and Cooper, 2000; Hanaoka et al., 2005; Liu et al., 2016), we believe that the role of *ZtYvh1* does not differ among these fungi. *ScYvh1* was demonstrated to be involved in 60S ribosomal subunit biogenesis, where it is recruited to the pre-60S to facilitate the release of the Mrt4 assembly factor from the ribosome stalk of the maturing 60S particles (Kemmler et al., 2009; Liu and Chang, 2009; Lo et al., 2009). Genes involved in ribosome biogenesis are regulated in response to environmental stresses (Gasch et al., 2000). *ScYvh1* mutants exhibit defective

60S ribosome biogenesis because the signal transduction delayed translation-competent 60S subunit affects the folding of nascent polypeptides and decoding of messenger RNA (Kemmler et al., 2009; Liu and Chang, 2009; Sacristan-Reviriego et al., 2015). We speculate that a similar mechanism leads to the impaired vegetative growth observed for the *ZtYvh1* mutants, especially during a temperature shift (Guan et al., 1992; Hanaoka et al., 2005; Sakumoto et al., 2002).

Another phenotype typically observed in *Yvh1* mutants is the hypersensitivity to cell-perturbing agents (Liu et al., 2016; Sacristan-Reviriego et al., 2015). The regulation of the Bck1-Mkk1-Slt2 MAPK

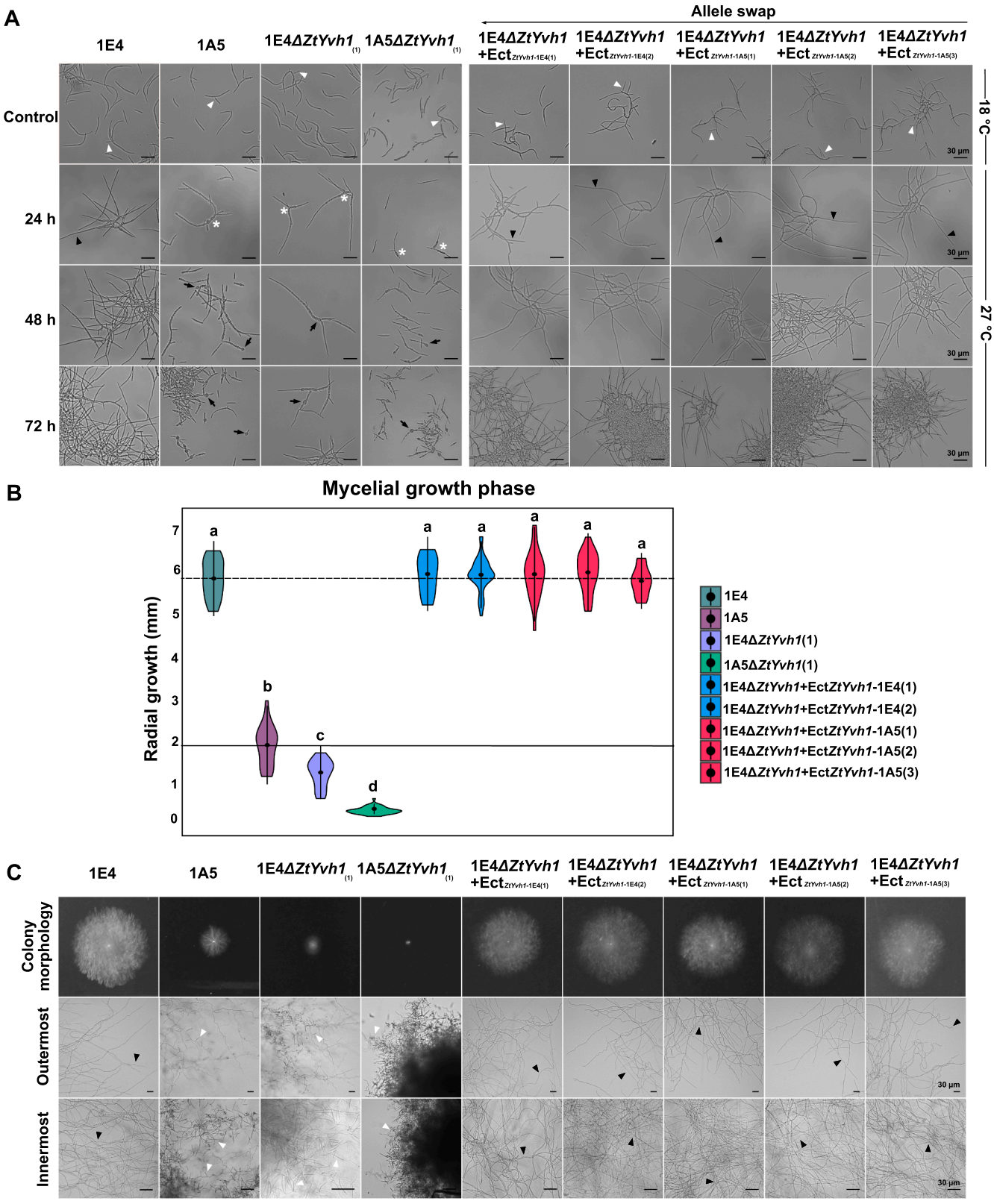

(caption on next page)

FIG. 4. *ZtYvh1* is required for hyphal growth. (A) Blastospores incubated on nutrient-rich YSB medium at 18°C (control environment) multiply by budding as blastospores (white triangles). The effect of heat stress on *Z. tritici* morphology was observed by exposing the strains at 27°C for 72 h. The 1E4 strain undergoes filamentation (black triangles), while 1A5 produces pseudohyphae (white asterisks) and chlamydospores (black arrows) as heat stress responses. Deletion of 1E4-*ZtYvh1* induced a similar response to 1A5, such as pseudohyphae (white asterisks) and chlamydospore (black arrows) formation under high temperatures. However, the 1A5Δ*ZtYvh1* null mutant did not differ from its 1A5 wild-type. Complementation of the 1E4Δ*ZtYvh1* mutant either with the 1E4- or 1A5-*ZtYvh1* allele restored the native filamentation (black triangles) of the 1E4 strain. All experiments were conducted independently three times with similar results. Numbers within brackets represent independent mutant lines. (B) Blastospores incubated on nutrient-limited WA at 18°C switch to hyphal growth. Violin plots demonstrate the radial growth (mm) of at least 20 colonies of each tested strain. The deletion of *ZtYvh1* strongly affects colony size independently of the genetic background. The ectopic integration of the 1E4- or 1A5-*ZtYvh1* allele into the 1E4Δ*ZtYvh1* mutant restored the 1E4 mycelial growth. The dashed or solid horizontal lines indicate the median of the radial growth (mm) of 1E4 and 1A5 strains, respectively. Different letters on the top of the bars indicate a significant difference among the tested strains according to Analysis of Variance (ANOVA). All experiments were conducted independently three times with similar results. (C) Overview images of colony morphology and light microscopies of the outermost and innermost regions of the colonies described in (B). Colonies from the 1A5- and 1E4Δ*ZtYvh1* mutants showed extensive blastosporulation resembling the 1A5 strain. The complemented 1E4-Ect$_{ZtYvh1\text{-}1E4}$ or 1E4-Ect$_{ZtYvh1\text{-}1A5}$ mutants restored the 1E4 mycelial growth phenotype. Black triangles point to hyphae and white triangles demonstrate areas of blastospore formation.

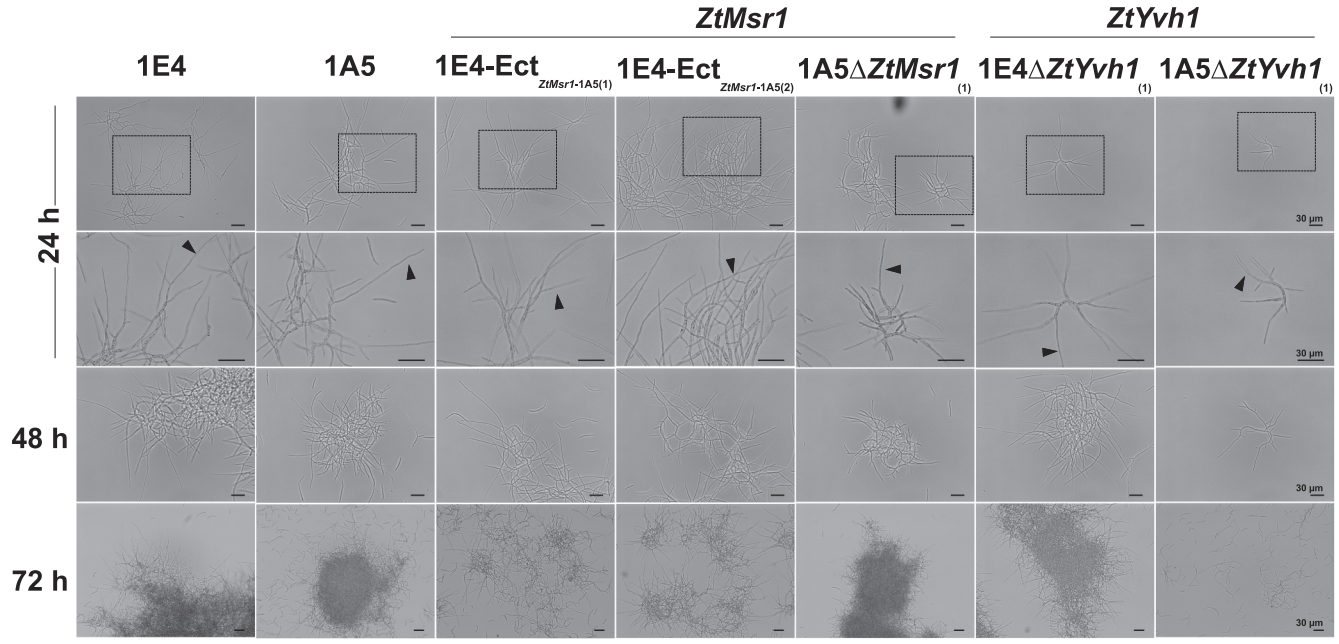

FIG. 5. Chlamydospore formation is a morphological response to the intracellular osmotic upshift generated during heat stress. Fungal spores were grown at 27°C for 72 h on YSB-supplemented with 1 M sorbitol. The ability of 1A5 and all mutant lines to produce chlamydospores as a temperature-dependent response was abolished. The 1A5 strain and the *ZtMsr1* and *ZtYvh1* derived mutant lines produced solely filamentation (black triangles) in this osmotic condition. All experiments were conducted independently three times with similar results. Numbers within brackets represent independent mutant lines.

cascade is thought to be crucial for CWI. In *M. oryzae*, *MoYvh1* functions in the maintenance of CWI via the regulation of the MAPK pathway (Liu et al., 2016). Consistent with the findings in *ΔMoYvh1*, the *ΔZtYvh1* null mutants were sensitive to both CR and SDS, suggesting that ZtYvh1 might be required for cell wall integrity in *Z. tritici*. Additionally, we showed that ZtMsr1 increases fungal perception to cell wall stresses, for example, the cell damage caused by increased temperature. While the 1E4-Ect$_{ZtMsr1\text{-}1A5}$ mutants were hampered by the CWI inhibitor CR, the deletion of *ZtMsr1* led to tolerance to this compound. Taking together all of the above-mentioned results, we suspect that activation of the CWI signaling pathway may allow the fungus to sense and respond to cell wall stresses that arise during a temperature upshift.

Upon heat stress, fungal cells accumulate trehalose, which protects native proteins against thermal-denaturation (Simola et al., 2000; Svanstrom and Melin, 2013), but also increases the intracellular osmolarity (Fillinger et al., 2001; Hottiger et al., 1987; Liu et al., 2021; Zaragoza et al., 1998). The cytoplasmic accumulation of this osmolyte compound causes hypotonic stress and turgor pressure which stretches the plasma membrane, a condition sensed by the Pck1 MAPK which in turn activates the CWI pathway (Davenport et al., 1995; Mensonides et al., 2005). Preventing trehalose synthesis diminishes CWI signaling during heat stress (Mensonides et al., 2005). In parallel, *Hog1* is rapidly phosphorylated through the Sho1-Pbs2-Hog1 MAPK cascade upon a temperature shift (Rodriguez-Pena et al., 2010; Winkler et al., 2002). Although the details of the cross-talk between the HOG and CWI pathways are not understood, mutants deleted in components of the CWI pathway are hypersensitive to heat stress. The deletion of *Slt2* is reported to promote large and swollen cells in oomycetes and filamentous fungi (Li et al., 2014; Onyilo et al., 2018; Yago et al., 2011), including in *Z. tritici* (Mehrabi et al., 2006a). We showed that these "swollen hyphae" in the *ZtSlt2* mutant are, in fact, chlamydospores. An earlier QTL study of temperature sensitivity in *Z. tritici* identified the *Pbs2* MAPK (Lendenmann et al., 2016), suggesting that the HOG pathway may also play a role in thermal adaptation in this fungus. The deletion of *ZtHog1* was earlier demonstrated to abolish the yeast-to-hyphae transition in *Z. tritici* (Mehrabi et al., 2006b). Here, we showed that deletion of *ZtHog1* induced chlamydospore formation, which supports our findings that filament-specific components need to be inactivated for the formation of chlamydospores, as demonstrated for the *ZtMsr1* and *ZtYvh1* mutants. The deletion of *Hog1* also causes osmosensitivity in different yeasts and filamentous fungi (Degols et al., 1996; Dixon et al., 1999; Park et al., 2004; San José et al., 1996), including in *Z. tritici* (Mehrabi et al., 2006b). Osmotic stabilization of the plasma membrane in the presence of a defective cell wall can prevent stimulation of the CWI pathway, and

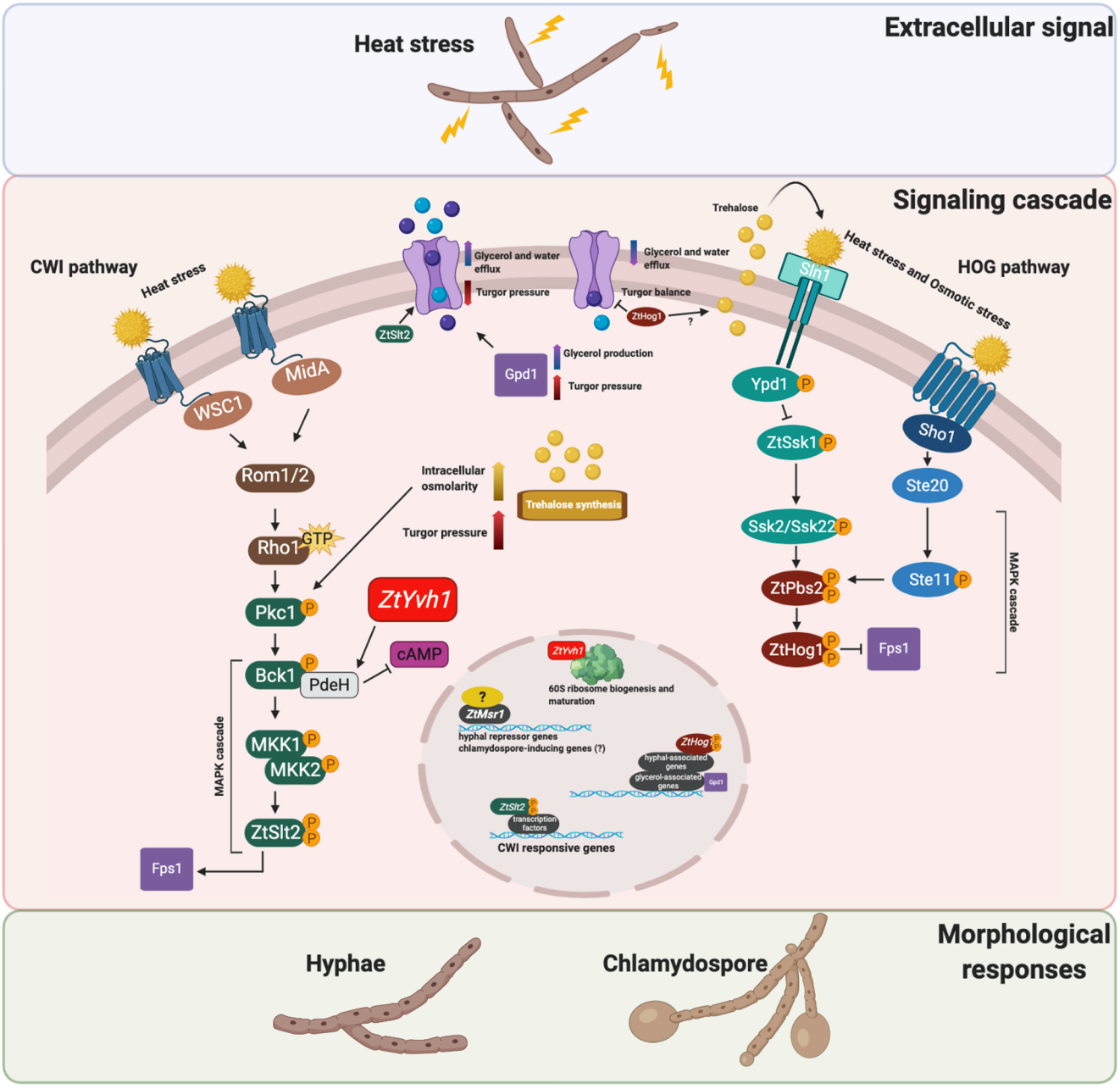

FIG. 6. A proposed model for the cross-talk between the CWI and the HOG pathways showing the contribution of *ZtMsr1* and *ZtYvh1* to temperature-dependent morphogenesis in *Zymoseptoria tritici*. Heat stress is known to induce accumulation of cytoplasmic trehalose, causing an increase in intracellular osmolarity and turgor pressure. The MAPK Pck1 from the cell wall integrity (CWI) pathway perceives this signal, which in turn activates downstream MAPK genes by phosphorylation. The phosphorylated-Slt2 is translocated into the nucleus and activates genes responsible for the maintenance of cell integrity. ZtMsr1 and ZtYvh1 contribute to morphological transitions in response to heat stress. Yvh1 has been previously demonstrated to activate the phosphodiesterase PdeH, which physically interacts with MAPK BcK1 from CWI and negatively regulates cAMP. Yvh1 also participates in the 60S ribosome biogenesis and maturation and thereby may contribute to the decoding of messenger RNAs affecting cellular processes in fungi, including vegetative growth. *Hog1* is activated via the Sho1-dependent pathway during heat stress. *ZtHog1* has also been demonstrated to be essential to activate hyphal-associated genes in *Z. tritici*. It has been proposed that *Hog1* contributes to the extracellular translocation of trehalose, although this mechanism is not yet understood. The efflux of trehalose is then perceived by Sln1, the second branch of the HOG pathway. The signaling through Sln1 activates Hog1, which in turn activates Gpd1 responsible for glycerol biosynthesis. The intracellular accumulation of glycerol also increases turgor pressure. To counterbalance the intracellular pressure, Slt2 phosphorylates Fps1, which opens the aquaporin water/glycerol channel to release glycerol and water. Once the normal osmotic conditions are reestablished, Hog1 phosphorylates Fps1 to close the channel. As demonstrated in this study, chlamydospore formation is suppressed in an osmotic stabilized environment, indicating that *Z. tritici* strains may perceive the intracellular osmolarity and turgor pressure differently, which in turn regulates the signaling cascade in a different manner resulting in hyphal or chlamydospore growth. Further studies will be required to pinpoint the cross talk between the CWI and HOG pathways, as well as to unveil the activation of the downstream signaling cascades and genes regulated by *ZtMsr1* and *ZtYvh1* during heat stress responses in *Z. tritici*. Image created with BioRender.com.

this would avert the regulatory cascade leading to hyphal or chlamydospore formation. Using an osmotic stabilized environment, we found that all the strains producing chlamydospores, including 1A5, underwent filamentation, except for the IPO323Δ*ZtHog1* mutant. Surprisingly, this MAPK mutant recovered its yeast-like growth in the osmotic stabilized condition, demonstrating that the intracellular osmotic stress and perception of turgor pressure are, in fact, the signal inducing chlamydospore formation through stimulating the CWI pathway; however, the induction of filamentation requires the integrity of HOG pathways in *Z. tritici*. This finding leads us to hypothesize that chlamydospores might be induced under any conditions that cause an osmotic upshift during the fungal lifecycle, in line with our previous discovery that chlamydospores are produced during the normal disease cycle of *Z. tritici* (Francisco et al., 2019). In summary, we conclude that *ZtMsr1* increases the perception of cell wall stresses, leading to inhibition of the formation of fungal hyphae under harmful conditions, such as when temperature rises – a condition that also causes fungal cell wall damage. In turn, when cell wall integrity is compromised, *ZtMsr1* can be activated and regulate the chlamydospore-inducing genes as a stress response survival strategy.

Our data illustrate the stunning complexity of mechanisms affecting temperature-dependent morphogenesis, highlighting the effects of naturally occurring genetic variants on the cross-regulation of MAPK signaling cascades. The results presented here provide a solid foundation for future studies on the intracellular processes driving morphological transitions in fungi. Despite some remaining questions, the general implication of our findings is clear: *ZtMsr1* and *ZtYvh1* contribute to temperature-dependent morphological responses in the fungal plant pathogen *Zymoseptoria tritici*.

CRediT authorship contribution statement

Carolina Sardinha Francisco: Conceptualization, Methodology, Investigation, Formal analysis, Writing – original draft, Project administration, Writing – review & editing. **Bruce A. McDonald:** Funding acquisition, Supervision, Writing – review & editing. **Javier Palma-Guerrero:** Conceptualization, Methodology, Project administration, Supervision, Writing – review & editing.

Declaration of Competing Interest

The authors declare that they have no known competing financial interests or personal relationships that could have appeared to influence the work reported in this paper.

Acknowledgements

This study was financed in part by the Coordenação de Aperfeiçoamento de Pessoal de Nível Superior – Brasil (CAPES) – Finance Code 001. We acknowledge Marc-Henri Lebrun from the French National Institute of Agricultural Research (INRAE) for kindly providing the MAPK mutants used in this study. We thank Michael Habig and Jason Rudd for the critical reading of the manuscript. We also thank Julien P. L. Alassimone, Dominik Vetsch, and Anja Kunz for their assistance with the experiments.

Appendix A. Supplementary material

Supplementary data to this article can be found online at https://doi.org/10.1016/j.fgb.2023.103811.

References

Abou-Gabal, M., Fagerland, J., 1980. Ultrastructure of the chlamydospore growth phase of *Aspergillus parasiticus* associated with higher production of aflatoxins. Mykosen 24, 307–311.
Arends, D., et al., 2010. R/qtl: high-throughput multiple QTL mapping. Bioinformatics 26, 2990–2992.
Arroyo, J., et al., 2016. Strengthening the fungal cell wall through chitin-glucan cross-links: effects on morphogenesis and cell integrity. Cell Microbiol. 18, 1239–1250.
Beeser, A.E., Cooper, T.G., 1999. The dual-specificity protein phosphatase Yvh1p acts upstream of the protein kinase Mck1p in promoting spore development in *Saccharomyces cerevisiae*. J. Bacteriol. 181, 5219–5224.
Beeser, A.E., Cooper, T.G., 2000. The dual-specificity protein phosphatase Yvh1p regulates sporulation, growth, and glycogen accumulation independently of catalytic activity in *Saccharomyces cerevisiae* via the cyclic AMP-dependent protein kinase cascade. J. Bacteriol. 182, 3517–3528.
Brown, A.J., et al., 2014. Stress adaptation in a pathogenic fungus. J. Exp. Biol. 217, 144–155.
Brown, A.J.P., et al., 2017. Stress Adaptation. Microbiol. Spectr. 5.
Cao, C., et al., 2020. Genome-wide identification for genes involved in sodium dodecyl sulfate toxicity in Saccharomyces cerevisiae. BMC Microbiol. 20, 34.
Chow, J., et al., 2018. Impact of fungal MAPK pathway targets on the cell wall. J. Fungi (Basel) 4.
Cousin, A., et al., 2006. The MAP kinase-encoding gene *MgFus3* of the non-appressorium phytopathogen *Mycosphaerella graminicola* is required for penetration and in vitro pycnidia formation. Mol. Plant. Pathol. 7, 269–278.
Couteaudier, Y., Alabouvette, C., 1990. Survival and inoculum potential of conidia and chlamydospores of *Fusarium oxysporum* f.sp. *lini* in soil. Can. J. Microbiol. 36, 551–556.
Davenport, K.R., et al., 1995. A second osmosensing signal transduction pathway in yeast. Hypotonic shock activates the Pck1 protein kinase-regulated cell integrity pathway. J. Biol. Chem. 270, 30157–30161.
Day, A.M., et al., 2018. Hog1 Regulates Stress Tolerance and Virulence in the Emerging Fungal Pathogen Candida auris. mSphere. 3, 13.
Degols, G., et al., 1996. Activation and regulation of the Spc1 stress-activated protein kinase in *Schizosaccharomyces pombe*. Mol. Cell. Biol. 16, 2870–2877.
Dixon, K.P., et al., 1999. Independent signaling pathways regulate cellular turgor during hyperosmotic stress and appressorium-mediated plant infection by *Magnaporthe grisea*. Plant Cell 11, 2045–2058.
Dunayevich, P., et al., 2018. Heat-stress triggers MAPK crosstalk to turn on the hyperosmotic response pathway. Sci. Rep. 8, 15168.
Falconer, D.S., 1996. Introduction to quantitative genetics. Pearson Education India.
Fillinger, S., et al., 2001. Trehalose is required for the acquisition of tolerance to a variety of stresses in the filamentous fungus *Aspergillus nidulans*. Microbiology 147, 1851–1862.
Francisco, C.S., et al., 2019. Morphological changes in response to environmental stresses in the fungal plant pathogen *Zymoseptoria tritici*. Sci. Rep. 9, 9642.
Fuchs, B.B., Mylonakis, E., 2009. Our paths might cross: the role of the fungal cell wall integrity pathway in stress response and cross talk with other stress response pathways. Eukaryot Cell. 8, 1616–1625.
Gancedo, J.M., 2001. Control of pseudohyphae formation in *Saccharomyces cerevisiae*. FEMS Microbioly Rev. 25, 107–123.
Gasch, A.P., et al., 2000. Genomic expression programs in the response of yeast cells to environmental changes. Mol. Biol. Cell 11, 4241–4257.
Gauthier, G.M., 2017. Fungal dimorphism and virulence: molecular mechanisms for temperature adaptation, immune evasion, and in vivo survival. Mediators Inflamm. 2017, 8491383.
Gey, U., et al., 2008. Yeast pyruvate dehydrogenase complex is regulated by a concerted activity of two kinases and two phosphatases. J. Biol. Chem. 283, 9759–9767.
Guan, K., et al., 1992. A yeast protein phosphatase related to the vaccinia virus VH1 phosphatase is induced by nitrogen starvation. Proc. Natl. Acad. Sci. U S A. 89, 12175–12179.
Guy, L., et al., 2010. genoPlotR: comparative gene and genome visualization in R. Bioinformatics 26, 2334–2335.
Habig, M., et al., 2020. The transcription factor Zt107320 affects the dimorphic switch, growth and virulence of the fungal wheat pathogen *Zymoseptoria tritici*. Mol. Plant Pathol. 21, 124–138.
Hanaoka, N., et al., 2005. A putative dual-specific protein phosphatase encoded by YVH1 controls growth, filamentation and virulence in *Candida albicans*. Microbiology 151, 2223–2232.
Heilmann, C.J., et al., 2013. Surface stress induces a conserved cell wall stress response in the pathogenic fungus *Candida albicans*. Eukaryot Cell. 12, 254–264.
Hohmann, S., 2002. Osmotic stress signaling and osmoadaptation in yeasts. Microbiol. Mol. Biol. Rev. 66, 300–372.
Hohmann, S., et al., 2007. Yeast Osmoregulation. Osmosens. Osmosignal. 29–45.
Hottiger, T., et al., 1987. Heat-induced accumulation and futile cycling of trehalose in *Saccharomyces cerevisiae*. J. Bacteriol. 169, 5518–5522.
Huang, Y.M., et al., 2021. *HOG1* has an essential role in the stress response, virulence and pathogenicity of *Cryptococcus gattii*. Exp. Ther. Med. 21, 476.
Jiang, C., et al., 2018. Mitogen-activated protein kinase signaling in plant pathogenic fungi. PLoS Pathog. 14, e1006875.
Kema, G.H., et al., 1996. Histology of the pathogenesis of *Mycosphaerella graminicola* in wheat. Biochem. Cell Biol. 86, 777–786.
Kema, G.H., van Silfhout, C.H., 1997. Genetic variation for virulence and resistance in the wheat-*Mycosphaerella graminicola* pathosystem III. Comparative seedling and adult plant experiments. Phytopathology 87, 266–272.
Kemmler, S., et al., 2009. *Yvh1* is required for a late maturation step in the 60S biogenesis pathway. J. Cell Biol. 186, 863–880.
Khang, C.H., et al., 2010. Translocation of *Magnaporthe oryzae* effectors into rice cells and their subsequent cell-to-cell movement. Plant Cell 22, 1388–1403.

Klein, B.S., Tebbets, B., 2007. Dimorphism and virulence in fungi. Curr. Opin. Microbiol. 10, 314–319.
Kock, C., et al., 2015. Up against the wall: is yeast cell wall integrity ensured by mechanosensing in plasma membrane microdomains? Appl. Environ. Microbiol. 81, 806–811.
Kopecká, M., Gabriel, M., 1992. The influence of Congo red on the cell wall and (1–3)-β-D-glucan microfibril biogenesis in *Saccharomyces cerevisiae*. Arch. Microbiol. 158, 115–126.
Krause-Buchholz, U., et al., 2006. YIL042c and YOR090c encode the kinase and phosphatase of the *Saccharomyces cerevisiae* pyruvate dehydrogenase complex. FEBS Lett. 580, 2553–2560.
Kumar, R., et al., 2004. A zinc-binding dual-specificity *YVH1* phosphatase in the malaria parasite, *Plasmodium falciparum*, and its interaction with the nuclear protein, pescadillo. Mol. Biochem. Parasitol. 133, 297–310.
Larochelle, M., et al., 2006. Oxidative stress-activated zinc cluster protein Stb5 has dual activator/repressor functions required for pentose phosphate pathway regulation and NADPH production. Mol. Cell Biol. 26, 6690–6701.
Larsson, A., 2014. AliView: a fast and lightweight alignment viewer and editor for large datasets. Bioinformatics 30, 3276–3278.
Leach, M.D., Cowen, L.E., 2013. Surviving the heat of the moment: a fungal pathogens perspective. PLoS Pathog. 9, e1003163.
Lendenmann, M.H., et al., 2014. Quantitative trait locus mapping of melanization in the plant pathogenic fungus *Zymoseptoria tritici*. G3 (Bethesda) 4, 2519–2533.
Lendenmann, M.H., et al., 2016. QTL mapping of temperature sensitivity reveals candidate genes for thermal adaptation and growth morphology in the plant pathogenic fungus *Zymoseptoria tritici*. Heredity (Edinb). 116, 384–394.
Levin, D.E., 2005. Cell wall integrity signaling in *Saccharomyces cerevisiae*. Microbiol. Mol. Biol. Rev. 69, 262–291.
Li, A., et al., 2014. PsMPK1, an SLT2-type mitogen-activated protein kinase, is required for hyphal growth, zoosporogenesis, cell wall integrity, and pathogenicity in *Phytophthora sojae*. Fungal Genet Biol. 65, 14–24.
Liu, X., et al., 2016. The putative protein phosphatase MoYvh1 functions upstream of MoPdeH to regulate the development and pathogenicity in *Magnaporthe oryzae*. Mol. Plant Microbe Interact. 29, 496–507.
Liu, Y., et al., 2021. Effect of osmotic stress on the growth, development and pathogenicity of *Setosphaeria turcica*. Front. Microbiol. 12, 706349.
Liu, Y., Chang, A., 2009. A mutant plasma membrane protein is stabilized upon loss of Yvh1, a novel ribosome assembly factor. Genetics 181, 907–915.
Lo, K.Y., et al., 2009. Ribosome stalk assembly requires the dual-specificity phosphatase Yvh1 for the exchange of Mrt4 with P0. J. Cell Biol. 186, 849–862.
Lu, J., et al., 2014. Systematic analysis of Zn2Cys6 transcription factors required for development and pathogenicity by high-throughput gene knockout in the rice blast fungus. PLoS Pathog. 10, e1004432.
MacPherson, S., et al., 2006. A fungal family of transcriptional regulators: the zinc cluster proteins. Microbiol. Mol. Biol. Rev. 70, 583–604.
Madden, K., et al., 1997. SBF cell cycle regulator as a target of the yeast PKC–MAP kinase pathway. Science 275, 1781–1784.
Martinez-Soto, D., Ruiz-Herrera, J., 2017. Functional analysis of the MAPK pathways in fungi. Rev. Iberoam Micol. 34, 192–202.
May, G.S., et al., 2005. Mitogen activated protein kinases of *Aspergillus fumigatus*. Med. Mycol. 43 (Suppl 1), S83–S86.
Mehrabi, R., et al., 2006a. MgSlt2, a cellular integrity MAP kinase gene of the fungal wheat pathogen Mycosphaerella graminicola, is dispensable for penetration but essential for invasive growth. Mol. Plant Microbe Interact. 19, 389–398.
Mehrabi, R., et al., 2006b. MgHog1 Regulates Dimorphism and Pathogenicity in the Fungal Wheat Pathogen Mycosphaerella graminicola. Mol. Plant Microbe Interact. 19, 1262–1269.
Mehrabi, R., et al., 2009. G(alpha) and Gbeta proteins regulate the cyclic AMP pathway that is required for development and pathogenicity of the phytopathogen *Mycosphaerella graminicola*. Eukaryot Cell. 8, 1001–1013.
Mehrabi, R., Kema, G.H., 2006. Protein kinase A subunits of the ascomycete pathogen *Mycosphaerella graminicola* regulate asexual fructification, filamentation, melanization and osmosensing. Mol. Plant Pathol. 7, 565–577.
Meile, L., et al., 2018. A fungal avirulence factor encoded in a highly plastic genomic region triggers partial resistance to septoria tritici blotch. New Phytol.
Mendiburu, F.D., Agricolae: Statistical Procedures for Agricultural Research. R Package Version 1.2-3. 2015.
Mensonides, F.I., et al., 2005. Activation of the protein kinase C1 pathway upon continuous heat stress in *Saccharomyces cerevisiae* is triggered by an intracellular increase in osmolarity due to trehalose accumulation. Appl. Environ. Microbiol. 71, 4531–4538.
Motteram, J., et al., 2011. Aberrant protein N-glycosylation impacts upon infection-related growth transitions of the haploid plant-pathogenic fungus *Mycosphaerella graminicola*. Mol. Microbiol. 81, 415–433.
Navarro-García, F., et al., 1995. Functional characterization of the *MKC1* gene of *Candida albicans*, which encodes a mitogen-activated protein kinase homolog related to cell integrity. Mol. Cell. Biol. 15, 2197–2206.
Nichols, C.B., et al., 2007. A Ras1-Cdc24 signal transduction pathway mediates thermotolerance in the fungal pathogen *Cryptococcus neoformans*. Mol. Microbiol. 63, 1118–1130.
Onyilo, F., et al., 2018. Silencing of the mitogen-activated protein kinases (MAPK) Fus3 and Slt2 in *Pseudocercospora fijiensis* reduces growth and virulence on host plants. Front. Plant Sci. 9, 291.
Palma-Guerrero, J., et al., 2017. Comparative transcriptome analyses in *Zymoseptoria tritici* reveal significant differences in gene expression among strains during plant infection. Mol. Plant Microbe Interact. 30, 231–244.
Panaretou, B., Zhai, C., 2008. The heat shock proteins: Their roles as multi-component machines for protein folding. Fungal Biol. Rev. 22, 110–119.
Park, S.M., et al., 2004. Characterization of HOG1 homologue, CpMK1, from *Cryphonectria parasitica* and evidence for hypovirus-mediated perturbation of its phosphorylation in response to hypertonic stress. Mol. Microbiol. 51, 1267–1277.
Philip, B., Levin, D.E., 2001. Wsc1 and Mid2 are cell surface sensors for cell wall integrity signaling that act through Rom2, a guanine nucleotide exchange factor for Rho1. Mol. Cell Biol. 21, 271–280.
Plissonneau, C., et al., 2018. Pangenome analyses of the wheat pathogen *Zymoseptoria tritici* reveal the structural basis of a highly plastic eukaryotic genome. BMC Biol. 16, 5.
Rodriguez-Pena, J.M., et al., 2010. The high-osmolarity glycerol (HOG) and cell wall integrity (CWI) signalling pathways interplay: a yeast dialogue between MAPK routes. Yeast 27, 495–502.
Roman, E., et al., 2020. The HOG MAPK pathway in *Candida albicans*: more than an osmosensing pathway. Int. Microbiol. 23, 23–29.
Rooney, P.J., Klein, B.S., 2002. Linking fungal morphogenesis with virulence. Cell. Microbiol. 4, 127–137.
Sacristan-Reviriego, A., et al., 2015. Identification of putative negative regulators of yeast signaling through a screening for protein phosphatases acting on cell wall integrity and mating MAPK pathways. Fungal Genet. Biol. 77, 1–11.
Sakumoto, N., et al., 2002. A series of double disruptants for protein phosphatase genes in *Saccharomyces cerevisiae* and their phenotypic analysis. Yeast 19, 587–599.
San José, A., et al., 1996. The mitogen-activated protein kinase homolog HOG1 gene controls glycerol accumulation in the pathogenic fungus *Candida albicans*. J. Bacteriol. 178, 5850–5852.
Sanz, A.B., et al., 2017. The CWI Pathway: Regulation of the Transcriptional Adaptive Response to Cell Wall Stress in Yeast. J. Fungi (Basel). 4.
Shapiro, R.S., Cowen, L.E., 2012. Uncovering cellular circuitry controlling temperature-dependent fungal morphogenesis. Virulence 3, 400–404.
Sil, A., Andrianopoulos, A., 2014. Thermally Dimorphic Human Fungal Pathogens-Polyphyletic Pathogens with a Convergent Pathogenicity Trait. Cold Spring Harb. Perspect. Med. 5, a019794.
Simola, M., et al., 2000. Trehalose is required for conformational repair of heat-denatured proteins in the yeast endoplasmic reticulum but not for maintenance of membrane traffic functions after severe heat stress. Mol. Microbiol. 37, 42–53.
Singer, M.A., Lindquist, S., 1998. Multiple effects of trehalose on protein folding *in vitro* and *in vivo*. Mol. Cell 1, 639–648.
Stecher, G., et al., 2020. Molecular Evolutionary Genetics Analysis (MEGA) for macOS. Mol. Biol. Evol. 37, 1237–1239.
Sudbery, P.E., 2011. Growth of *Candida albicans* hyphae. Nat. Rev. Microbiol. 9, 737–748.
Svanstrom, A., Melin, P., 2013. Intracellular trehalase activity is required for development, germination and heat-stress resistance of *Aspergillus niger* conidia. Res. Microbiol. 164, 91–99.
Thompson, D.S., et al., 2011. Coevolution of morphology and virulence in *Candida* species. Eukaryot Cell. 10, 1173–1182.
Tiwari, S., et al., 2015. Role of Heat-Shock Proteins in Cellular Function and in the Biology of Fungi. Biotechnol. Res. Int. 2015, 132635.
Torriani, S.F., et al., 2015. *Zymoseptoria tritici*: A major threat to wheat production, integrated approaches to control. Fungal Genet. Biol. 79, 8–12.
Verna, J., et al., 1997. A family of genes required for maintenance of cell wall integrity and for the stress response in *Saccharomyces cerevisiae*. Proc. Natl. Acad. Sci. U S A. 94, 13804–13809.
Veses, V., Gow, N.A., 2009. Pseudohypha budding patterns of *Candida albicans*. Med. Mycol. 47, 268–275.
Wang, L., Lin, X., 2012. Morphogenesis in fungal pathogenicity: shape, size, and surface. PLoS Pathog. 8, e1003027.
Whiteway, M., Bachewich, C., 2007. Morphogenesis in *Candida albicans*. Annu. Rev. Microbiol. 61, 529–553.
Wickham, H., 2009. ggplot2: Elegant Graphics for Data Analysis. Use R. Springer-Verlag, New York.
Winkler, A., et al., 2002. Heat stress activates the yeast high-osmolarity glycerol mitogen-activated protein kinase pathway, and protein tyrosine phosphatases are essential under heat stress. Eukaryot Cell. 1, 163–173.
Yago, J.I., et al., 2011. The SLT2 mitogen-activated protein kinase-mediated signalling pathway governs conidiation, morphogenesis, fungal virulence and production of toxin and melanin in the tangerine pathotype of *Alternaria alternata*. Mol. Plant Pathol. 12, 653–665.
Yin, Z., et al., 2016. Phosphodiesterase MoPdeH targets MoMck1 of the conserved mitogen-activated protein (MAP) kinase signalling pathway to regulate cell wall integrity in rice blast fungus *Magnaporthe oryzae*. Mol. Plant Pathol. 17, 654–668.
Zaragoza, O., et al., 1998. Disruption of the *Candida albicans TPS1* gene encoding trehalose-6-phosphate synthase impairs formation of hyphae and decreases infectivity. J. Bacteriol. 180, 3809–3815.
Zhan, J., et al., 2002. Distribution of mating type alleles in the wheat pathogen *Mycosphaerella graminicola* over spatial scales from lesions to continents. Fungal Genet. Biol. 36, 128–136.

Zhan, J., et al., 2005. Variation for neutral markers is correlated with variation for quantitative traits in the plant pathogenic fungus *Mycosphaerella graminicola*. Mol. Ecol. 14, 2683–2693.
Zhao, X., et al., 2007. Mitogen-activated protein kinase pathways and fungal pathogenesis. Eukaryot Cell. 6, 1701–1714.
Zhao, X., et al., 2018. Gene expression related to trehalose metabolism and its effect on *Volvariella volvacea* under low temperature stress. Sci. Rep. 8, 11011.
Zhong, Z., et al., 2017. A small secreted protein in *Zymoseptoria tritici* is responsible for avirulence on wheat cultivars carrying the Stb6 resistance gene. New Phytol. 214, 619–631.